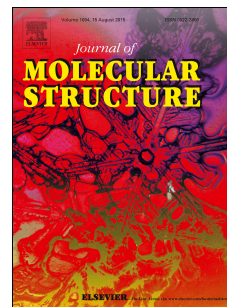


Accepted Manuscript

Photochromic properties of the molecule Azure A chloride in polyvinyl alcohol matrix

Siyamak Shahab, Liudmila Filippovich, Rakesh Kumar, Mahdieh Darroudi, Mostafa Yousefzadeh Borzehandani, Maryam Gomar, Fatemeh Haji Hajikolaee



PII: S0022-2860(15)30195-2

DOI: [10.1016/j.molstruc.2015.08.007](https://doi.org/10.1016/j.molstruc.2015.08.007)

Reference: MOLSTR 21739

To appear in: *Journal of Molecular Structure*

Received Date: 19 May 2015

Revised Date: 2 August 2015

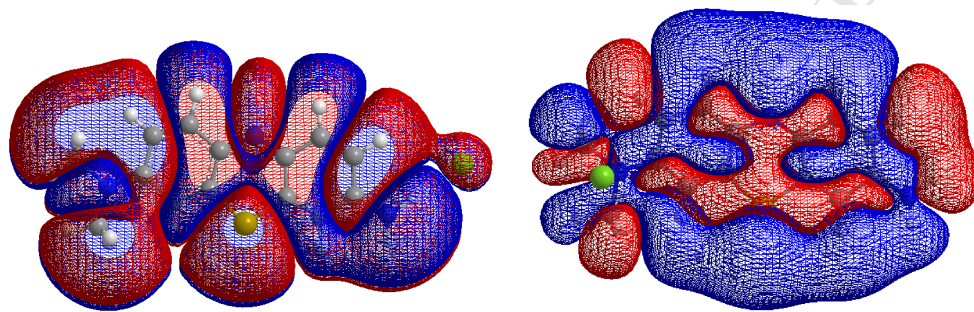
Accepted Date: 3 August 2015

Please cite this article as: S. Shahab, L. Filippovich, R. Kumar, M. Darroudi, M.Y. Borzehandani, M. Gomar, F.H. Hajikolaee, Photochromic properties of the molecule Azure A chloride in polyvinyl alcohol matrix, *Journal of Molecular Structure* (2015), doi: 10.1016/j.molstruc.2015.08.007.

This is a PDF file of an unedited manuscript that has been accepted for publication. As a service to our customers we are providing this early version of the manuscript. The manuscript will undergo copyediting, typesetting, and review of the resulting proof before it is published in its final form. Please note that during the production process errors may be discovered which could affect the content, and all legal disclaimers that apply to the journal pertain.

Graphical Abstract

This work relates to a polyfunctional polymer PVA films containing photosensitive photochromic organic dye. It also provide the possibility of combining them to create a heat-polymer film of sun screen materials from a variable (adaptive) light transmittance in the visible region of the spectrum depending on the intensity of solar radiation for use in construction, automotive and aviation industries for glazing large skylights. Study of the anisotropy of thermal conductivity allows you to select the substance which can more easily conduct heat flux and in the meantime not warm when you use the sun.



Sub: Submission of manuscript for full paper in Journal of Molecular Structure

Dear Sir,

Please find herewith the enclosed manuscript:

Article title

Photochromic properties of the molecule Azure A chloride in polyvinyl alcohol matrix

The name of journal

Journal of Molecular Structure

The author's affiliations with full postal address

Siyamak Shahab

Institute of Physical Organic Chemistry

National Academy of Sciences of Belarus, 13 Surganov Str., Minsk 220072

E-mail: siyamak.shahab@yahoo.com

Liudmila Filippovich

Institute of Physical Organic Chemistry

National Academy of Sciences of Belarus, 13 Surganov Str., Minsk 220072

E-mail: luda1977@list.ru

Rakesh Kumar

Department of Applied Sciences

CTIEMT, CT Group of Institutions, Jalandhar-144020 (Punjab) India.

E-mail: rakesh_nitj@yahoo.co.in

Mob. No. +91-9888 982369

Mahdieh Darroudi

Department of Organic Chemistry

Faculty of Chemistry, University of Mazandaran, Babolsar, Iran 47416.

E-mail: mahdie_darroudi@yahoo.com

Mostafa Yousefzadeh Borzehandani

Department of Organic Chemistry, Faculty of Chemistry, University of Mazandaran, 47416 Babolsar, Iran

E-mail: jan_1989@ymail.com

Maryam Gomar

Department of Chemistry, University of Yasouj, 75914-353, Yasouj, Iran

Fatemeh Haji Hajikolaee

Tajan High Education Institute, 47617-96486, Ghaemshahr, Mazandaran, Iran

E-mail: Fatima7_56@yahoo.com

Photochromic properties of the molecule Azure A chloride in polyvinyl alcohol matrix

Siyamak Shahab^a, Liudmila Filippovich^a, Rakesh Kumar^{b,c}, Mahdieh Darroudi^d, Mostafa Yousefzadeh Borzehandani^e, Maryam Gomar^f, Fatemeh Haji Hajikolae^g

^a*Institute of Physical Organic Chemistry, National Academy of Sciences of Belarus, 13 Surganova Str, Minsk 220072*

^b*Department of Applied Sciences, CTIT, CT Group of Institutions, Jalandhar-144020 (Punjab) India.*

^c*Department of Chemistry, Dr B R Ambedkar National Institute of Technology, Jalandhar-144011 (Punjab) India.*

^d*Department of Organic Chemistry, University of Mazandaran, 47416 Babolsar, Iran*

^e*Department of Chemistry, Islamic Azad University-Rasht Branch, P.O. Box 41335-3516, Rasht, Iran*

^f*Department of Chemistry, University of Yasouj, 75914-353, Yasouj, Iran*

^g*Tajan High Education Institute, 47617-96486, Ghaemshahr, Mazandaran, Iran*

ABSTRACT

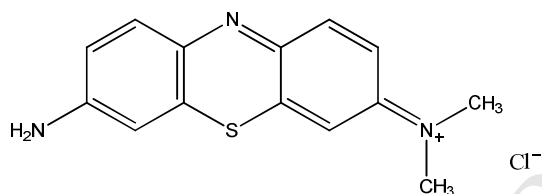
In the present work, isomerization, photophysical properties and heat conductivity of the substance Azure A chloride (AZAC): 3-amino-7-(dimethylamino)phenothiazin-5-ium chloride under the action of UV radiation in the presence of polyvinyl alcohol (PVA) matrix was studied using the Hartree-Fock (HF) and Density Functional Theory (DFT) methods. The electronic absorption spectra of AZAC in dimethylformamide (DMF) solution and in aqueous medium before and after UV radiation were calculated. The nature of absorption bands of AZAC and its tautomeric prototropic form with the transfer of the electron (AZAC₁) in the visible and near UV spectral regions was interpreted. The solvent effect on the absorption spectrum of the AZAC has established. The comparison of measured FTIR, UV-Visible data allowed assignments of major special features of title molecules. The frontier molecular orbital HOMO-LUMO have been also presented that shows the charge transfer interactions taking place within these molecules. The excitation energies for both molecules AZAC and AZAC₁ have also been calculated. The experimental as well as theoretical investigations of azure molecule have a close agreement and it gives other important clues about the properties of the system. Anisotropy of thermal conductivity in PVA-films containing AZAC and AZAC₁ were also measured.

Keywords: DFT studies, UV and IR spectra, UV radiation, anisotropy, Thermal conductivity

Corresponding authors: rakesh_nitj@yahoo.co.in (R. Kumar); Mob. No. 9888982369
siyamak.shahab@yahoo.com (S. Shahab)

1. Introduction

AZAC is a phenothiazine dye available as green to brown powder. It is formed by the oxidation of methylene blue and is strongly metachromatic. It is utilized as a part of making azure eosin stains for blood smear staining. Azure dyes are used as redox mediators for electrochemical biosensing [1].



Azure A chloride is generally used as solvents and colored reagents in numerous experimental and scientific investigations [2]. Estimation of the molecular orbital geometry demonstrate that the visible absorption maxima of such type of molecules correspond to the electron transition from highest occupied molecular orbital (HOMO) to the lowest unoccupied molecular orbital (LUMO). The structure and the vibrational spectroscopic investigation of the thiazines are critical for the understanding of their physicochemical and pharmaceutical properties. Vibrational spectroscopic studies of thiazine dye and its derivatives have been reported in the literature [3]. The solvent effect is closely related to the nature and degree of dye-solvent interactions. The impact of solvent on the aggregate formation of a wide variety of ionic dyes has also been reported by many researchers [4]. The present investigations expect to understand the structural and bonding features and molecular information such as π conjugations, electron delocalization and resonance interaction using UV-Vis calculations. In the prior study, FT-Raman, IR as well as UV-VIS spectra of the phenothiazine dye AZAC have been recorded and examined [1]. The authors have also reported the ability of the TD - DFT method to predict the absorption spectra of a series of oxazine dyes and the effect of solvent on the accuracy of these predictions [5]. Taking into the account of this study, it's clear that in the series of oxazine dyes an accurate prediction of the excitation energy requires the inclusion of solvent. A spectrophotometric method for ascertaining the presence of anionic detergent in milk using azure A dye is described in literature [6]. In the previous research vibrational assignments for the observed Raman bands, based on the computed potential energy distribution (PED) and isotopic shifts were made [7]. First time, azure B has been used as achromogenic reagent for the spectrophotometric determination of product. The proposed method, which is simple and rapid, offers the advantages of sensitivity and wide range of determinations without the need for

extraction or heating and it does not involve any stringent reaction conditions [8]. Excited electronic states of molecular systems can be calculated by TD DFT and TD HF methods [9-15].

Density functional theory is conceptually and computationally very similar to HF theory, but it provides vastly improved results and has outcome turned into an exceptionally prevalent technique. The aim of the current work is to study photophysical properties (photochromism, isomerization) and anisotropy of thermal conductivity in colored stretched PVA-films by *ab initio* (HF, DFT), UV/Vis- and IR-Spectroscopies and Indicator methods for determination of Thermal Conductivity of polymer films.

2. Experimental

2.1 Reagent and Physical measurements

All chemical were used of analytical reagent grade. Used PVA «Mowiol 28-99» manufactured by the Hoëchst Com. (Germany). Experimental UV-Vis spectrum of the compound was recorded on UV-Visible Spectrophotometer Cary 300 (Varian, USA). Experimental IR spectrum of films was recorded in the frequency region 400-4000 cm^{-1} on a spectrophotometer of Protégé 460 (Nicolet, US).

Photostability of films was studied using unfiltered radiation of high-pressure Hg-lamp DRSH-1000. The intensity of light falling perpendicular to the surface of the sample was 0.009 W/cm^2 . At an exposure temperature of sample was 20-22 °C. The absorption spectra of the films were measured before and after radiation. Heat conductivity of films was measured on the complex equipment LC – 201 using indicator method of determining the heat conductivity of polymer materials.

2.2 Preparation

PVA films were prepared from 10% PVA solutions, containing the AZAC, gelling and plasticizing agents [16]. The films were cast on the polished glasses and dried in the closed box at temperature 20-22 °C. Uniaxial orientation was done in the 4% boric acid (H_3BO_3) solution at 42-45 °C. The washed film was dried for 30 min at temperature 60-63 °C. The value of stretching degree (R_s) was determined as the ratio between the length of the films after and before uniaxial stretching. The thickness of the resulting films was between 50 to 55 μm .

3. Computational details

The theoretical molecular structures of AZAC and AZAC₁ in the ground state were optimized by HF/6-31G*, HF/6-311G* and DFT/B3LYP/6-311G* levels of theory in DMF and aqueous

medium. Theoretical absorption spectra of the molecules optimized in solvents (DMF and water) were calculated using TDHF/6-31G*, TDHF/6-311G* and TDB3LYP/6-311G* methods. To account solvent effect Polarized Continuum Model (PCM) was used. The theoretical IR spectrum of optimized molecules was calculated using the DFT/B3LYP/6-311G* method. The scaling factor for the level of the theory is 0.98. The input files of both molecules were prepared by Gauss View and also used for the visualization of the structure and simulated vibrational and UV spectrum [17]. All the calculations are carried out using Gaussian 09 package [18].

4. Results and discussion

4.1 Geometric structure of AZAC and AZAC₁

The geometry of the molecules AZAC and AZAC₁ has been optimized DFT/B3LYP/6-311G* levels of theory (Figure 1). The calculated structural parameters bond lengths and bond angles of the molecules are presented in Table S1& S2.

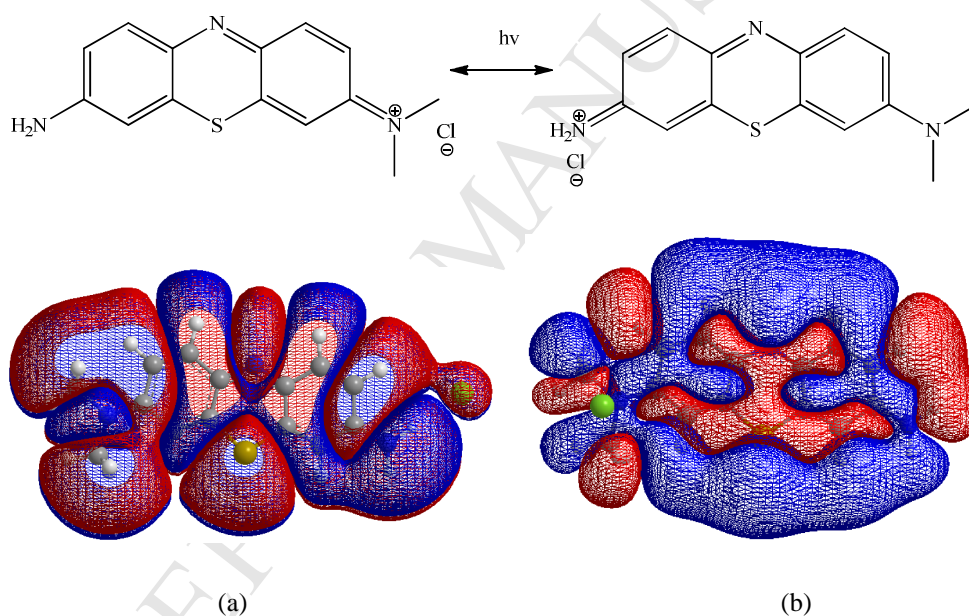


Fig. 1 Optimized molecular structures of (a) AZAC and (b) AZAC₁

4.2. Electronic spectrum

Experimental and theoretical calculations demonstrate that AZAC molecule is very sensitive to the presence of solvents due to a total charge of its molecule, and it reacts with a solvent and change the absorption spectrum of AZAC. Calculated absorption spectra of AZAC in water, DMF and experimental spectra of AZAC in water are presented (Fig. 2). In the transition from water to DMF, absorption peak in the UV region does not undergo a large change, while in the visible region hypsochromic shift with absorption band occur at 128nm. The experimental

spectrum has a strong absorption band in the range 598-633 nm which is characterized by maxima at 633 nm (Fig. 2c). DFT calculations of AZAC show maximum absorption at 630 nm ($f = 1.9$). This absorption band is belonged to the transition into the excited singlet state S_1 and describes by a wave function corresponding to a superposition of three configurations for one-electron excitations ($73 \rightarrow 77$, $76 \rightarrow 77$ and $77 \rightarrow 76$) (Table 1).

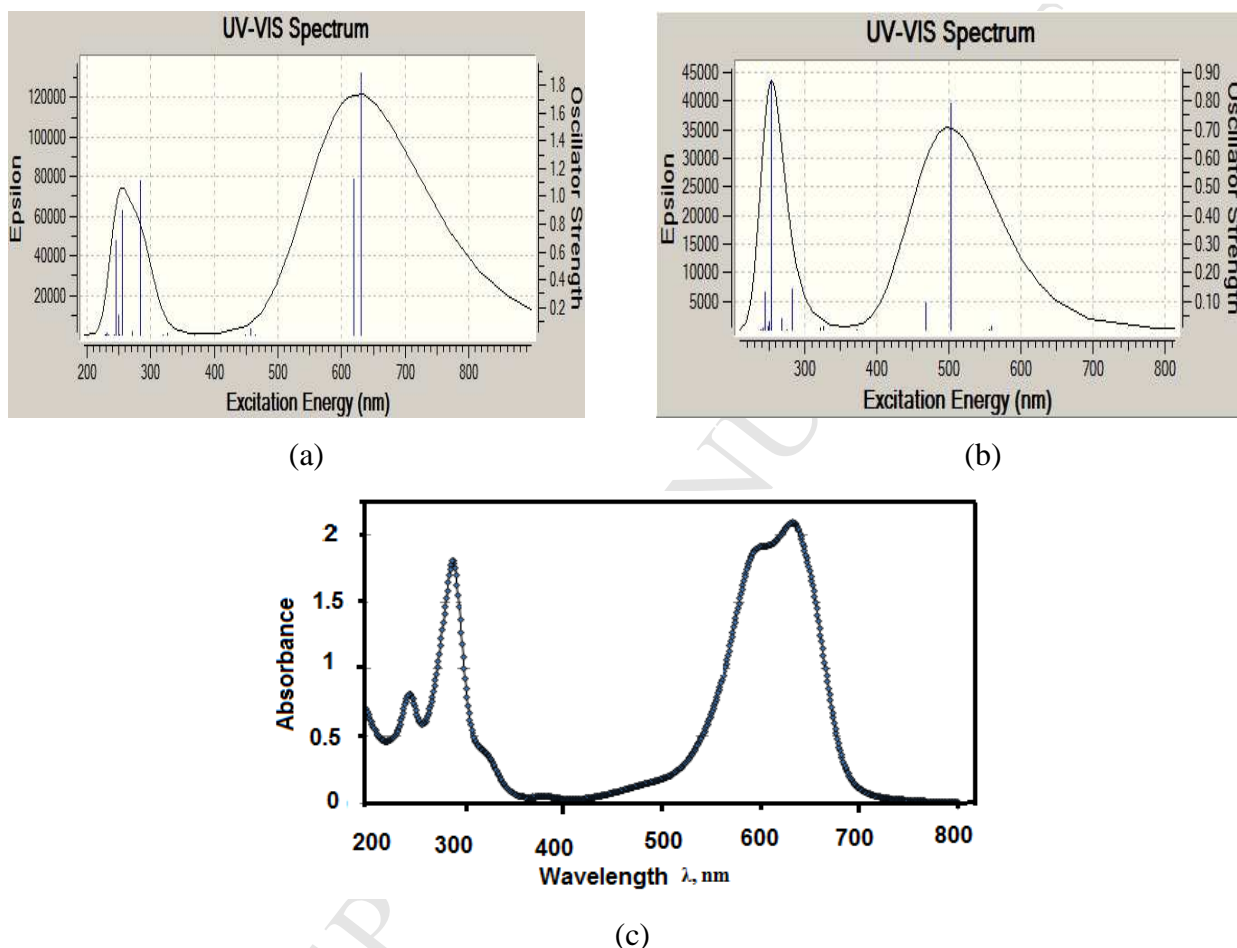


Fig. 2. Absorption spectrum Calculated (a) - in water, (b) – in DMF) and (c) Experimental UV-Vis spectrum of AZAC in water at concentration $3.0 \cdot 10^{-5}$ M/l

Excitation of an electron from molecular orbitals 76 to 77 are the main contributor for the formation of the electronic spectrum at 630 nm (Fig. 3). It is clear from the MO (76) in which electron cloud is localized in the centre of molecule and also around the S atom where the high density of the electron cloud is observed. In MO 77, electron cloud is localized around the S atom and also on the entire length of the molecule.

The experimental UV spectrum shows absorption threshold at about 614 nm whereas calculated absorption band occur at 619 nm ($f = 1.1$). This absorption band is belonged to the transition into the excited singlet state S_2 and describe by a wave function corresponding to a superposition of two configurations for one-electron excitations ($73 \rightarrow 77$ and $75 \rightarrow 77$) (Table. 1 & Fig. 3).

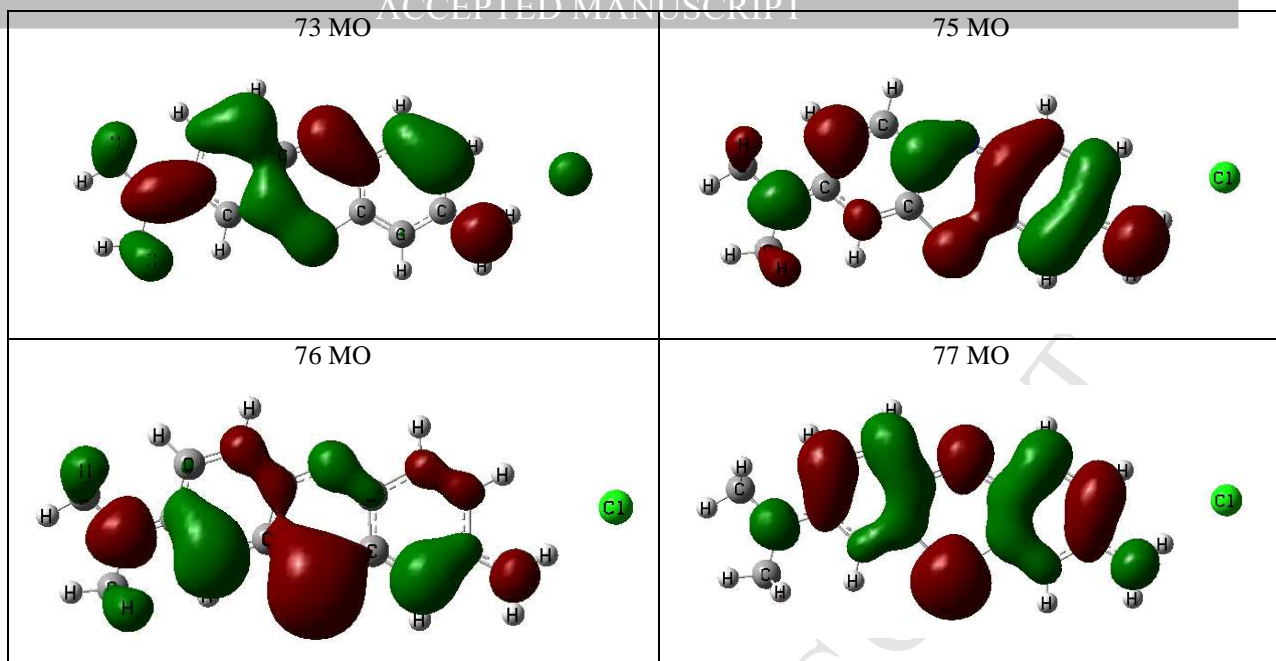


Fig. 3 Molecular orbitals involved in formation of absorption spectrum of AZAC at $\lambda = 630$ and 619 nm.

Theoretical calculations don't show absorption band at 598 nm but it appears in the experimental spectrum that may be associated with a relative error of spectrophotometer. In the UV region of spectrum DFT calculations show a peak of absorption at 285 nm whereas experimental spectrum has an absorption band at 287 nm. This absorption band is belonged to the transition into the excited singlet state S_9 and describes by a wave function corresponding to a superposition of four configurations for one-electron excitations ($71 \rightarrow 77$, $76 \rightarrow 78$, $76 \rightarrow 79$ and $76 \rightarrow 80$) (Table. 1).

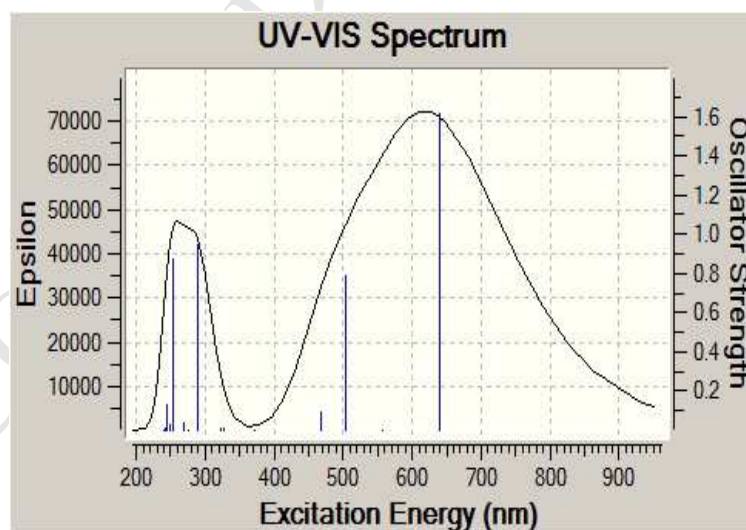
In the transition from AZAC to AZAC1 under UV radiation appears photochromism. In our case the photochromic effect must be due to a reversible electron transfer inside the molecule. Calculated spectrum of AZAC1 in water is presented in Figure. 4. The calculated spectrum shows absorption at 639 nm ($f = 1.6$). This absorption bond is belonged to the transition into the excited singlet state S_1 and describes by a wave function corresponding to a superposition of three configurations for one-electron excitations ($73 \rightarrow 77$, $75 \rightarrow 77$ and $76 \rightarrow 77$) (Table. 2). Excitation of an electron from molecular orbitals MOs $73 - 77$ are the main contributor to the formation of the electronic spectrum at 639 nm. It can be seen that in 73 MO electron cloud is localized to the benzene rings and around the S atom of the molecule AZAC₁. Around the S atom high density of the electron cloud is observed. In 77 MO electron cloud is localized to the S atom and central part of the molecule.

In visible region has the one peak at 503 nm. This absorption bond is belongs to the transition into the excited singlet state S_4 that described by a wave function corresponding to a superposition of four configurations for one-electron excitations ($72 \rightarrow 77$, $73 \rightarrow 77$, $76 \rightarrow 77$ and $77 \rightarrow 76$) (Fig.5).

Table 1. The calculated electronic spectrum of AZAC

λ (nm)	Decomposition of the wave functions at once excited configuration	Oscillator strength (f)
630	73 \rightarrow 77	0.10575
	76 \rightarrow 77	0.69771
	76 \leftarrow 77	-0.10612
619	73 \rightarrow 77	-0.19542
	75 \rightarrow 77	0.67331
465	74 \rightarrow 77	0.70478
458	73 \rightarrow 77	0.66425
	75 \rightarrow 77	0.20527
	76 \rightarrow 77	-0.10188
448	72 \rightarrow 77	0.70464
369	70 \rightarrow 77	0.70509
326	69 \rightarrow 77	0.10075
	71 \rightarrow 77	0.63725
	76 \rightarrow 78	0.24658
320	69 \rightarrow 77	0.69440
285	71 \rightarrow 77	-0.20063
	76 \rightarrow 78	0.62181
	76 \rightarrow 79	-0.10255
	76 \rightarrow 80	0.19473
271	73 \rightarrow 78	-0.21804
	75 \rightarrow 78	0.20610
	76 \rightarrow 79	0.60755

In the UV region of spectrum DFT calculations show a peak of absorption at 290 nm. This absorption band belongs to the transition into the excited singlet state S_9 and described by a wave function corresponding to a superposition of four configurations for one-electron excitations (71 \rightarrow 77, 76 \rightarrow 78 and 76 \rightarrow 80) (Table. 2).

**Fig. 4.** Calculated UV-Vis spectrum of AZAC₁ in water

By comparing the absorption spectra of AZAC to AZAC₁ in water was found the following facts:

- (1) Excited state 1 (S_1): Bathochromic shift at 9 nm (630 \rightarrow 639 nm) with increasing in the oscillator strength at 0.2.
- (2) Excited state 2 (S_2): The peak of absorption at 619 nm disappears in

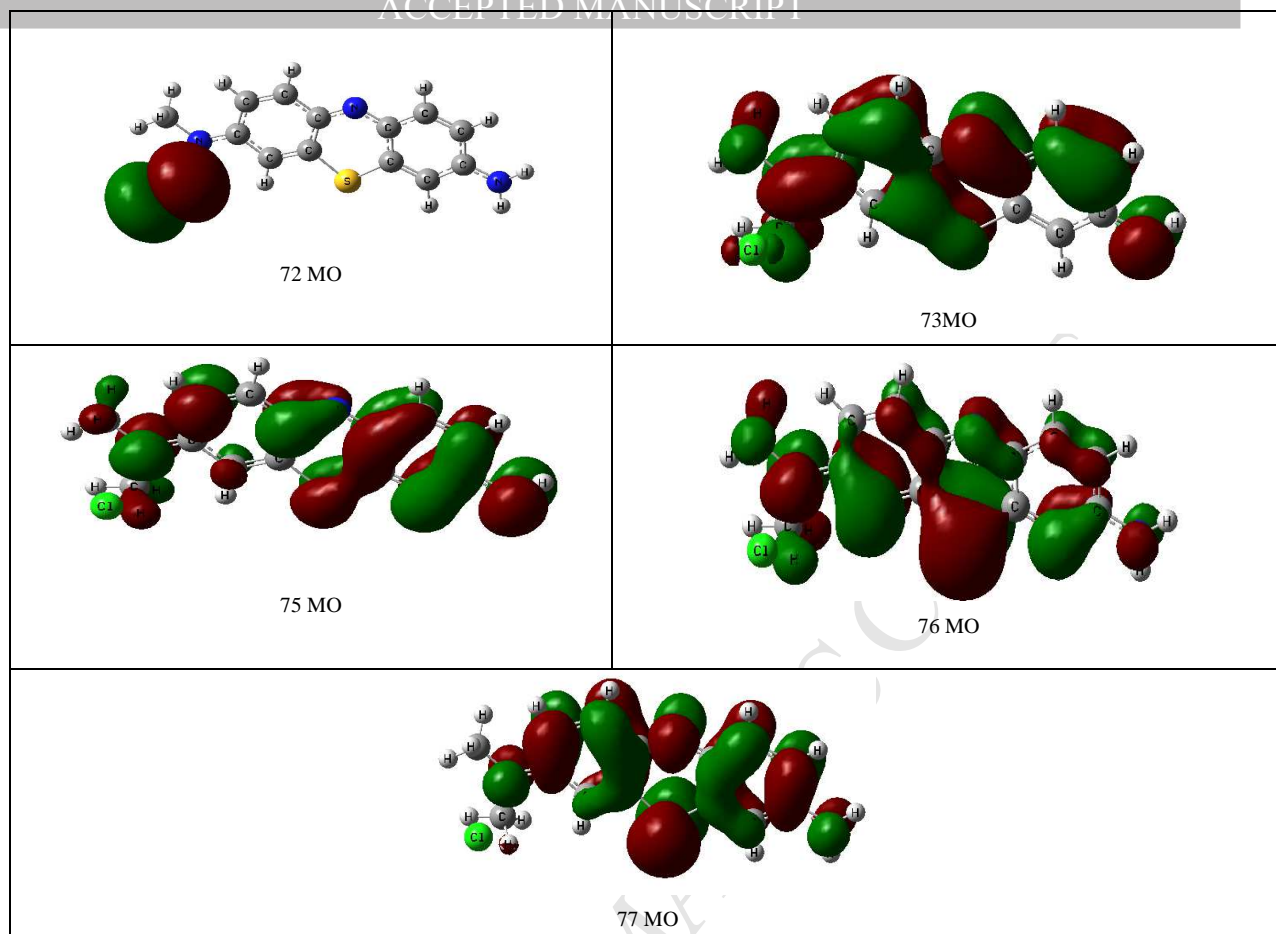


Fig. 5 Molecular orbitals involved in formation of absorption spectrum of the AZAC₁ at $\lambda = 639$ and 503 nm.

electronic spectrum of AZAC₁. There is a new absorption peak at 557 nm, but the transition is forbidden by symmetry. (3) Excited state 4 (S4): Bathochromic shift at 45 nm with increasing in

Table 2. Selected molecular orbital transitions, excitation energies and oscillator strengths of AZAC₁

λ (nm)	Decomposition of the wave functions at once excited configuration					Oscillator strength (f)			
639	73 -> 77	0.61183,	75 -> 77	-0.30611,	76 -> 77	-0.16522	1.6		
557	73 -> 77	0.29184,	74 -> 77	-0.10102,	75 -> 77	0.63357	0.0		
556	73 -> 77	0.10869,	74 -> 77	0.69552			0.0		
503	72 -> 77	0.15180,	73 -> 77	0.16512,	76 -> 77	0.66687,	76 -> 77	-0.10288	0.8
468	72 -> 77	0.68203,	76 -> 77	-0.14904			0.0		
372	70 -> 77	0.70524					0.0		
326	69 -> 77	0.29473,	71 -> 77	0.59251,	76 -> 78	-0.20457	0.0		
321	69 -> 77	0.63601,	71 -> 77	-0.26175,	76 -> 78	0.12155	0.0		
290	71 -> 77	0.19083,	76 -> 78	0.62836,	76 -> 80	0.19087	0.9		
276	73 -> 78	-0.49077,	75 -> 78	0.49588			0.0		

the oscillator strength at 0.8. (4) Excited state 9 (S9): Bathochromic shift at 5 nm with decreasing in the oscillator strength at 0.2. The results of calculations of electronic spectra of AZAC and AZAC₁ in water and DMF with different methods and basis sets are given in Table 3.

Table 3. Comparison of *ab initio* methods (TDHF and TDDFT) and various basis sets for calculation of absorption peaks of AZAC and AZAC₁ in water and DMF

Method	AZAC in aqueous medium	AZAC in DMF	AZAC ₁ in aqueous medium	AZAC ₁ in DMF
TDHF/6-31G*	561, 505, 488, 465, 403, 356, 348, 366, 307, 284	523, 505, 478, 466, 440, 377, 354, 316, 309, 290	573, 561, 523, 501, 486, 450, 434, 403, 355, 291	560, 551, 507, 475, 458, 460, 423, 401, 376, 301
TDHF/6-311G*	545, 412, 338, 313, 296, 260, 254, 231, 209, 192	510, 504, 483, 451, 444, 403, 382, 380, 356, 286	576, 555, 501, 488, 471, 390, 366, 352, 301, 288	506, 500, 471, 434, 404, 401, 390, 367, 307, 254
TDB3LYP/6-311G*	630, 619, 465, 458, 448, 369, 326, 320, 285, 271	502, 485, 461, 442, 428, 383, 352, 341, 309, 252	639, 557, 556, 503, 468, 372, 326, 322, 290, 276	580, 564, 555, 506, 496, 432, 376, 370, 333, 312

By comparing the calculated and experimental data we have found that B3LYP/6-311G* method is better than the other methods that predicts changes in the absorption spectrum of AZAC.

4.3. UV radiation of PVA-films

In order to study photochromic properties of AZAC, their PVA film was prepared. The absorption spectrum of the sample was recorded after one hour UV radiation. The absorption spectrum of the sample was recorded again after 24 and 72 hours. During the time, the sample was placed in a dark (vacuum). It is seen that initial PVA film containing AZAC (curve 1) transfers to AZAC₁ (curve 2) after one hour radiation (Fig. 6). The peak of absorption does not change ($\lambda = 640$ nm). Over time (curves 3,4) the optical density of the sample begins to grow (for curve 2: $D = 0.10$, for curve 3: $D = 0.36$). This indicates that the reduction reaction is reversible to AZAC. After 6 days AZAC fully recovered and we have the curve 1 again.

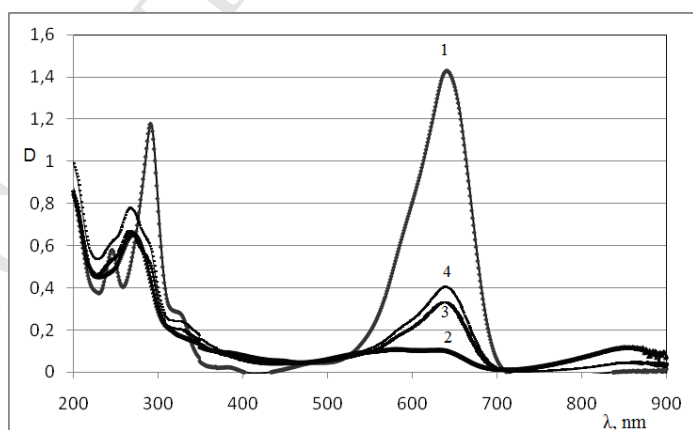


Fig. 6 Experimental UV spectrum of film containing AZAC (1) – Initial film before radiation, (2) – after one hour radiation, (3) – after 24 hours, (4) – after 72 hours.

In order to confirm the accuracy of our findings, IR spectroscopy was used. The observed and calculated spectra of both AZAC & AZAC₁ are found to be in good agreement with each other.

Simulated results show that the theoretical spectrum reproduces the experimental one with their main characteristics (Table. 4, Fig S3& S4).

Comparison of the IR spectra of AZAC and AZAC₁ has shown some important characteristics:

1. 1708.88 cm⁻¹ (stretching vibrations of NH₂) and 2910.73 cm⁻¹ (stretching vibrations of R-N⁺≡C) indicates the presence of AZAC.
2. 1376.74 cm⁻¹ (stretching vibrations of -NH₂⁺), 1708.29 cm⁻¹ (stretching vibrations of -NH₂⁺ salt), 2940.89 cm⁻¹ (stretching vibrations of -NH₂⁺). Based on the IR spectra of both compounds it is concluded that there is a transformation of AZAC to AZAC₁ during UV irradiation of the samples.

Table 4. Experimental and calculated vibrational frequencies and their assignment of AZAC and AZAC₁ by using B3LYP/6-311G* method

AZAC			AZAC ₁		
v _{exp} (cm ⁻¹)	v _{calc} (cm ⁻¹)	Assignment	v _{exp} (cm ⁻¹)	v _{calc} (cm ⁻¹)	Assignment
421.54	445.76	vibrations of methylene rocking	422.61	435.45	bending vibrations of =C-H aromatic
480.02	488.01	bending vibrations of =C-H aromatic	479.85	489.06	bending vibrations of =C-H (out-of-plane)
663.66	673.56	bending vibrations of =C-H (out-of-plane)	663.23	669.78	bending vibrations of =C-H aromatic
852.34	841.11	bending vibrations of RCH=CR'R''	852.25	870.01	bending vibrations of =C-H aromatic
917.98	898.08	bending vibrations of =C-H aromatic	917.93	905.34	S-C=CH
1093.48	1080.46	S-C=CH	1093.70	1075.21	stretching vibrations of C-N
1142.86	1222.57	stretching vibrations of C-N	1142.75	1131.68	stretching vibrations of C-N -Nme ₂ ⁺
1237.35	1205.43	stretching vibrations of C-N Nme ₂	1237.73	1245.80	stretching vibrations of C=C of the aromatic ring
1331.27	1370.09	bending vibrations of methylene	1331.67	1312.59	stretching vibrations of C=C of the aromatic ring
1377.46	1385.61	bending vibrations of methylene	1376.74	1365.12	stretching vibrations of -NH ₂ ⁺
1425.00	1449.31	bending vibrations of methylene	1425.67	1433.77	stretching vibrations of C=C of the alkene
1603.22	1600.36	stretching vibrations of C=C of the aromatic ring	1662.98	1654.04	stretching vibrations of C=N
1662.87	1626.62	stretching vibrations of C=C of the aromatic ring	1708.29	1721.72	stretching vibrations of NH ₂ ⁺ salt
1708.88	1689.66	stretching vibrations of NH ₂	2335.94	2356.15	stretching vibrations of C-H aliphatic
2910.73	2896.84	stretching vibrations of R-N ⁺ ≡C	2911.06	2932.74	stretching vibrations of C-H aromatic
2941.28	2965.86	stretching vibrations of C-H aromatic	2940.89	2967.18	stretching vibrations of -NH ₂ ⁺ aromatic
3382.89	3360.12	-NH ₂ aromatic	3382.72	3387.09	-NH ₂ aromatic

4.4. Anisotropy of thermal conductivity of PVA-films.

During chemical photochromism many properties of the system like refractive index, solubility, viscosity and thermal conductivity changes. In the present work, we have studied thermal conductivity of the PVA-AZAC and PVA-AZAC₁ systems. In the earlier research reports, special paints were used to sharply change the initial color at a critical temperature (T_{cr}). The isothermal surface moves at a certain speed in the proportion to a local gradient of the temperature field. Thermo-physical characteristics of the material can be judged by the speed of isotherm movement and the form of flowing surface.

Thermal indicators of small sizes at small T_{cr} were used to avoid thermal destruction of polymer material. Firstly, thermal indicator is putting on a film by a thin layer and at regular intervals by a draw plate. Then, after some drying period its colored surface contacts to (30 sec.) a heat metal needles (it is heated up approximately to 55 °C). Thermo-physical properties of the films were determined by heat conductivity of samples in parallel ($\lambda_{||}$) and perpendicular (λ_{\perp}) directions of stretching axis. In case of anisotropic materials an ellipse is drawn. During this work, it was established that the oriented PVA-films is the phenomenon of *anisotropy of thermal conductivity* ($\lambda_{||} / \lambda_{\perp}$). Thermal conductivity in a ($\lambda_{||}$) direction is higher than as compared to their perpendicular orientations (λ_{\perp}).

It has been noticed that during thermal expansion and thermal conductivity, geometric parameters of molecule and intermolecular forces play a significant role. In unstretched PVA-films anisotropy of thermal conductivity is not observed appreciably ($\lambda_{||} = 0,875$; $\lambda_{\perp} = 0,869$ W/m.°C) whereas in stretched PVA-films it is noticed very clearly (Table. 5). When we inject the dye in PVA-film there is change in its thermal conductivity (Table. 6). It has been found that along an axis of orientation, it increases, whereas in perpendicular direction it reduces. Results of thermal conductivity measurements of PVA-films containing AZAC and AZAC₁ depending on stretching degree (Table. 6).

Table 5. Dependence of thermal conductivity on stretching degree in pure PVA-films

R_s	λ , W/ m.°C		
	$\lambda_{ }$	λ_{\perp}	$\lambda_{ } / \lambda_{\perp}$
1.5	0.876	0.764	1.15
2	0.878	0.636	1.38
2.5	0.880	0.549	1.60
3	0.881	0.503	1.75
4	0.882	0.475	1.86

Table 6. Thermal conductivity of PVA-films containing AZAC and AZAC₁ at concentration 0.2 wt.%

Dye	R _s	λ , W/ m.°C		
		λ_{\parallel}	λ_{\perp}	$\lambda_{\parallel} / \lambda_{\perp}$
AZAC	2	0.865	0.254	3.40
	3	0.851	0.240	3.55
	4	0.844	0.216	3.91
	5	0.840	0.186	4.52
AZAC ₁	2	0.866	0.202	4.29
	3	0.853	0.173	4.93
	4	0.849	0.147	5.78
	5	0.837	0.109	7.68

The obtained data suggest that in the PVA-AZAC₁ system, anisotropy of thermal conductivity is stronger than in the PVA - AZAC system. In some photochromic compounds we have found that the isomers which are less stable (have a larger energy system) have a greater anisotropy of thermal conductivity as compared with the more stable isomers. Theoretical calculation of the full energies of AZAC and AZAC₁ by DFT/B3LYP/6-311G* levels of theory lead to the following values: HF_{AZAC} = -1564.5995599 and HF_{AZAC₁} = -1564.5897449.

5. Conclusions

In the present paper, geometric parameters, electronic and IR spectra of the molecules Azure A chloride (AZAC) 3-amino-7-(dimethylamino)phenothiazin-5-ium chloride and its tautomeric prototropic form with the transfer of the electron (AZAC₁) by DFT and HF methods using 6-31G*, 6-311G* basis sets were calculated. UV-Vis absorption spectra were analyzed via experimental and theoretical calculation (TD HF, TD DFT) methods. Photochromic properties of the AZAC appear as a result of UV radiation was also established. In stretched PVA-films containing AZAC are phenomena of anisotropy of thermal conductivity. The full energies of AZAC and AZAC₁ by DFT/B3LYP/6-311G* were also calculated. This study suggests that isomers which are less stable have a greater anisotropy of thermal conductivity as compared to those which is more stable.

Acknowledgement

One of the author Dr. Rakesh Kumar is highly thankful to Dr. B R Ambedkar National Institute of Technology, Jalandhar for providing the research infrastructure to carry out the theoretical work present in the manuscript.

References

- [1] M. Snehalatha, I. Hubert Joe, C. Ravikumar and V. S. Jayakumar, *J. Raman Spectrosc.* 40 (2009) 176-182.
- [2] M. Havelcova, P. Kubat b, I. Nemcova, *Dyes and Pigments* 44 (2000) 49-54.
- [3] A. Mills, D. Hazafy, J. Parkinson, T. Tuttle, M. G. Hutchings, *Dyes and Pigments* 88 (2011) 149-155.
- [4] K. Lawrence, W.J. Panzardi P.J. Panzardi, *J. of Analytical Chemistry* 47(1975) 1742-1745.
- [5] S. Fleming, A. Mills, T. Tuttle, *Beilstein Journal of Organic Chemistry* 7 (2011) 432-441.
- [6] A.K. Barui, R. Sharma, Y.S. Rajput, *International Dairy Journal* 24 (2012) 44-47.
- [7] D. Pan, D. L. Phillips, *J. Phys. Chem. A* 103 (1999) 4737-4743.
- [8] **B. Narayana, T. Cherian**, *J. Braz. Chem. Soc.* 16 (2005) 978-981.
- [9] (a) K. Hara, M. Kurashige, Y. Dan-Oh, C. Kasada, A. Shinpo, S. Suga, K. Sayama, H. Arakawa, *New J. Chem.* 27 (2003)783-785. (b) S. Shahab, H. A. Almodarresiyeh, R. Kumar, M. Darroudi, *J. Mol. Struct.* 1088 (2015) 105–110. (c) S. Shahab, R. Kumar, M. Darroudi, M. Y. Borzehandani, *J. Mol. Struct.* 1083 (2015) 198–203.
- [10] T. Horiuchi, H. Miura, K. Sumioka, S. Uchida, *J. Am. Chem. Soc.* 126 (2004) 2218-12219.
- [11] N. Kaumura, Z. Wang, S. Mori, M. Miashita, E. Suzuki, K. Hara, *J. Am. Chem. Soc.* 128, (2006) 14256-14257.
- [12] M. Cossi, N. Rega, G. Scalmani, V. Barone, *J. Comput. Chem.* 24 (2003) 669-681.
- [13] H.A. Almodarresiyeh, S.N. Shahab, V.M. Zelenkovsky, V.E. Agabekov, *J. of App. Spect.* 81 (2014) 181-183.
- [14] H.A. Almodarresiyeh, S.N. Shahab, V.M. Zelenkovsky, N.G. Ariko, L.N. Filippovich, V.E. Agabekov, *J. of App. Spect.* 81 (2014) 42-47.
- [15] J. Fabian, *J. Dyes and Pigments* 84 (2010) 36-53.
- [16] L.N. Filippovich, N.G. Ariko, H.A. Almodarresiyeh, S.N. Shahab, P.M. Malashko, V.E. Agabekov. *J. Semiconductor Physics, Quantum Electronics and Optoelectronics.* 16 (2013) 220-223.
- [17] A. Frisch, A. B. Nielsen, A. J. Holder, *Gauss View Users Manual*, Gaussian Inc., 2008.
- [18] M. J. Frisch, G. W. Trucks, H. B. Schlegel, G. E. Scuseria, M. A. Robb, et al., *Gaussian 09*, Revision A.02, Gaussian Inc., Wallingford, CT, 2009.

Highlights

- Optimization of Azure A chloride
- UV-Vis and IR spectra were recorded and compared with calculated ones
- Charge transfer occur within the molecules
- Preparation of polarizing films

ACCEPTED MANUSCRIPT

Supplementary Data

Table S1. Optimized geometric parameters of AZAC with HF/6-31G*, HF/6-311G* and B3LYP/6-311G* methods

Parameter	Method		
	HF/6-31G*	HF/6-311G*	B3LYP/6-311G*
Bond length (Å)			
C(18)-H(32)	1.0773	1.0823	1.0901
C(18)-H(31)	1.0841	1.0823	1.0979
C(18)-H(30)	1.0840	1.0756	1.0979
C(17)-H(29)	1.0774	1.0820	1.0901
C(17)-H(28)	1.0837	1.0819	1.0974
C(17)-H(27)	1.0837	1.0756	1.0974
N(16)-C(18)	1.4561	1.4606	1.4574
N(16)-C(17)	1.4574	1.4621	1.4586
C(15)-H(26)	1.0703	0.9913	1.0833
C(14)-N(16)	1.3427	1.3531	1.3686
C(14)-C(15)	1.4116	1.4267	1.4150
C(13)-H(25)	1.0697	1.0497	1.0825
C(13)-C(14)	1.4299	1.3431	1.4286
C(12)-H(24)	1.0738	1.0711	1.0853
C(12)-C(13)	1.3548	1.4425	1.3730
C(11)-C(15)	1.3749	1.3750	1.3899
C(10)-C(12)	1.4167	1.4170	1.4191
C(10)-C(11)	1.4141	1.4264	1.4238
N(9)-C(10)	1.3370	1.3046	1.3584
S(8)-C(11)	1.7455	1.3646	1.7574
N(7)-H(23)	1.0060	1.0071	1.1002
N(7)-H(22)	0.9968	1.0109	1.0140
C(6)-H(21)	1.0733	1.0734	1.0852
C(5)-N(9)	1.2966	1.3078	1.3162
C(5)-C(6)	1.4422	1.4246	1.4471
C(4)-S(8)	1.7371	1.7456	1.7562
C(4)-C(5)	1.4463	1.4219	1.4602
C(3)-H(20)	1.0742	1.0741	1.0874
C(3)-C(4)	1.3607	1.3722	1.3700
C(2)-N(7)	1.3133	1.3142	1.3173
C(2)-C(3)	1.4193	1.4050	1.4332
C(1)-H(19)	1.0730	1.0736	1.0886
C(1)-C(6)	1.3402	1.3493	1.3539
C(1)-C(2)	1.4404	1.4274	1.4510
Bond angle (°)	HF/6-31G*	HF/6-311G*	B3LYP/6-311G*
H(32)-C(18)-H(31)	108.1750	109.2515	108.0595
H(32)-C(18)-H(30)	108.1718	108.2794	108.0621
H(32)-C(18)-N(16)	108.9874	111.0333	109.1735
H(31)-C(18)-H(30)	108.8573	108.2520	108.3789
H(31)-C(18)-N(16)	111.2765	111.0182	111.5210
H(30)-C(18)-N(16)	111.2731	108.9226	111.5247
H(29)-C(17)-H(28)	108.1333	109.3177	108.0088
H(29)-C(17)-H(27)	108.1359	108.2263	108.0108
H(29)-C(17)-N(16)	108.8392	111.1415	109.0178
H(28)-C(17)-H(27)	108.9210	108.1976	108.4429
H(28)-C(17)-N(16)	111.3511	111.1286	111.6147
H(27)-C(17)-N(16)	111.3537	108.7356	111.6167
C(18)-N(16)-C(17)	118.7912	118.2054	119.3494
C(18)-N(16)-C(14)	120.4744	120.5498	120.2560
C(17)-N(16)-C(14)	120.7343	120.2215	120.3946
H(26)-C(15)-C(14)	120.2548	120.2566	120.2533
H(26)-C(15)-C(11)	118.9241	118.8601	118.8380
C(14)-C(15)-C(11)	120.8212	120.8605	120.9087
N(16)-C(14)-C(15)	121.2245	121.5177	121.1431
N(16)-C(14)-C(13)	120.9374	121.0014	121.0045
C(15)-C(14)-C(13)	117.8380	117.8621	117.8524
H(25)-C(13)-C(14)	120.2672	120.2200	120.2187
H(25)-C(13)-C(12)	119.1478	119.1312	119.1195
C(14)-C(13)-C(12)	120.5850	120.5748	120.6618

H(24)-C(12)-C(13)	120.3938	120.6356	120.8833
H(24)-C(12)-C(10)	117.4656	117.0056	116.8225
C(13)-C(12)-C(10)	122.1406	122.2693	122.2941
C(15)-C(11)-C(10)	121.4621	121.4601	121.4600
C(15)-C(11)-S(8)	117.8024	117.7533	117.7238
C(10)-C(11)-S(8)	120.7355	120.7706	120.8162
C(12)-C(10)-C(11)	117.1531	117.0104	116.8229
C(12)-C(10)-N(9)	117.6982	117.5127	117.1886
C(11)-C(10)-N(9)	125.1487	125.8071	125.9885
C(10)-N(9)-C(5)	125.2813	124.8467	123.8098
C(11)-S(8)-C(4)	103.2681	103.2361	103.2281
H(23)-N(7)-H(22)	117.4223	117.8690	119.8412
H(23)-N(7)-C(2)	121.6244	120.1284	120.2741
H(22)-N(7)-C(2)	120.9532	120.6904	119.8847
H(21)-C(6)-C(5)	116.7081	116.0022	115.9616
H(21)-C(6)-C(1)	121.1836	121.5698	121.4699
C(5)-C(6)-C(1)	122.1083	122.4457	122.5684
N(9)-C(5)-C(6)	117.4711	117.7011	117.2437
N(9)-C(5)-C(4)	125.2983	125.0948	125.9317
C(6)-C(5)-C(4)	117.2305	117.5876	116.8246
S(8)-C(4)-C(5)	120.2680	120.2957	120.2257
S(8)-C(4)-C(3)	118.7761	118.7609	118.7392
C(5)-C(4)-C(3)	120.9558	120.9988	121.0351
H(20)-C(3)-C(4)	120.8793	120.6941	120.6641
H(20)-C(3)-C(2)	118.8125	118.7733	118.6681
C(4)-C(3)-C(2)	120.3082	120.4840	120.6678
N(7)-C(2)-C(3)	120.8625	121.9336	122.4497
N(7)-C(2)-C(1)	119.4546	119.1148	118.4326
C(3)-C(2)-C(1)	119.6829	119.3406	119.1177
H(19)-C(1)-C(6)	121.7617	121.3362	123.2816
H(19)-C(1)-C(2)	118.5241	118.0031	116.9321
C(6)-C(1)-C(2)	119.7142	118.9253	119.7863

Table S2. Optimized geometric parameters of AZAC₁ by HF/6-31G*, HF/6-311G* and B3LYP/6-311G* methods

Parameter	Method		
	HF/6-31G*	HF/6-311G*	B3LYP/6-311G*
Bond length (Å)			
N(18)-H(32)	1.0029	1.0125	1.0106
N(18)-H(31)	1.1134	1.0108	1.0103
C(17)-N(18)	1.3389	1.3561	1.3446
C(16)-H(30)	1.0843	1.0991	1.0854
C(16)-C(17)	1.4321	1.4328	1.4331
C(15)-H(29)	1.0797	1.0833	1.0849
C(15)-C(16)	1.3656	1.3696	1.3641
C(14)-H(28)	1.0874	1.0822	1.0861
C(14)-C(17)	1.4233	1.4203	1.4147
C(13)-C(14)	1.3867	1.3870	1.3829
C(12)-C(15)	1.4366	1.4359	1.4320
C(12)-C(13)	1.4483	1.4461	1.4413
N(11)-C(12)	1.3352	1.3367	1.3378
S(10)-C(13)	1.7627	1.7614	1.7502
C(9)-H(27)	1.0912	1.0901	1.0886
C(9)-H(26)	1.0912	1.0922	1.0939
C(9)-H(25)	1.0932	1.0989	1.0956
C(8)-H(24)	1.0845	1.0860	1.0885
C(8)-H(22)	1.0992	1.0911	1.0945
N(7)-C(9)	1.4683	1.4702	1.4668
N(7)-C(8)	1.4694	1.4680	1.4652
C(6)-H(21)	1.0820	1.0833	1.0850
C(5)-H(20)	1.0798	1.0849	1.0816
C(5)-C(6)	1.3538	1.3599	1.3630
C(4)-N(7)	1.3490	1.3526	1.3500
C(4)-C(5)	1.4466	1.4423	1.4404
C(3)-H(19)	1.0888	1.0851	1.0824
C(3)-C(4)	1.4341	1.4300	1.4231
C(2)-S(10)	1.7618	1.7606	1.7516
C(2)-C(3)	1.3856	1.3834	1.3811
C(1)-N(11)	1.3362	1.3344	1.3339
C(1)-C(6)	1.4340	1.4312	1.4320
C(1)-C(2)	1.4389	1.4417	1.4418
Bond angle (°)	HF/6-31G*	HF/6-311G*	B3LYP/6-311G*
H(32)-N(18)-H(31)	117.1117	117.1102	117.1052
H(32)-N(18)-C(17)	121.4890	121.3971	121.5498
H(31)-N(18)-C(17)	121.7740	121.6609	121.3448
N(18)-C(17)-C(16)	120.2205	120.0001	119.9678
N(18)-C(17)-C(14)	120.7199	120.7203	120.7177
C(16)-C(17)-C(14)	119.6001	119.5670	119.3145
H(30)-C(16)-C(17)	119.3618	119.1202	119.1114
H(30)-C(16)-C(15)	120.7729	120.7701	120.7652
C(17)-C(16)-C(15)	120.1289	120.1264	120.1234
H(29)-C(15)-C(16)	121.1300	121.1241	121.1229
H(29)-C(15)-C(12)	116.9012	116.9002	116.8960
C(16)-C(15)-C(12)	121.9220	121.8831	121.9811
H(28)-C(14)-C(17)	119.1820	119.2332	119.1326
H(28)-C(14)-C(13)	120.8933	120.6440	120.5500
C(17)-C(14)-C(13)	120.6793	120.6678	120.3174
C(14)-C(13)-C(12)	121.1107	121.1223	121.1174
C(14)-C(13)-S(10)	118.2294	118.2226	118.1566
C(12)-C(13)-S(10)	120.8561	120.8320	120.7259
C(15)-C(12)-C(13)	117.2797	117.3349	117.1462
C(15)-C(12)-N(11)	117.1229	117.1005	117.0883
C(13)-C(12)-N(11)	125.6709	125.3101	125.7655
C(12)-N(11)-C(1)	123.9866	123.8556	123.7249
C(13)-S(10)-C(2)	103.7699	103.5611	103.2355
H(27)-C(9)-H(26)	108.1602	108.1791	108.1708
H(27)-C(9)-H(25)	108.5123	108.5094	108.5101
H(27)-C(9)-N(7)	108.7109	108.7110	108.7050
H(26)-C(9)-H(25)	109.4001	109.3966	109.3995

H(26)-C(9)-N(7)	110.9598	110.9568	110.9572
H(25)-C(9)-N(7)	111.0115	111.1100	111.0176
H(24)-C(8)-H(23)	109.0021	108.5322	108.5388
H(24)-C(8)-H(22)	108.4424	108.2998	108.3015
H(24)-C(8)-N(7)	108.9056	108.9100	108.9071
H(23)-C(8)-H(22)	109.2196	109.2311	109.2234
H(23)-C(8)-N(7)	110.9126	110.9101	110.9085
H(22)-C(8)-N(7)	110.9015	110.8976	110.8915
C(9)-N(7)-C(8)	118.4202	118.4188	118.4154
C(9)-N(7)-C(4)	120.8673	120.8660	120.8631
C(8)-N(7)-C(4)	120.5076	120.5031	120.5099
H(21)-C(6)-C(5)	120.8353	120.8407	120.8396
H(21)-C(6)-C(1)	116.5541	116.7430	116.8877
H(20)-C(5)-C(6)	119.2193	119.2284	119.2253
H(20)-C(5)-C(4)	120.1103	120.0586	120.0305
C(6)-C(5)-C(4)	120.8670	120.7374	120.7433
N(7)-C(4)-C(5)	120.8633	120.8602	120.8534
N(7)-C(4)-C(3)	121.1940	121.1894	121.1770
C(5)-C(4)-C(3)	118.1121	118.0045	117.9696
H(19)-C(3)-C(4)	120.1196	120.1010	120.0029
H(19)-C(3)-C(2)	119.1631	119.1504	119.0548
C(4)-C(3)-C(2)	120.7739	120.8834	120.9421
S(10)-C(2)-C(3)	118.0795	118.0882	118.0685
S(10)-C(2)-C(1)	120.5294	120.5237	120.5311
C(3)-C(2)-C(1)	121.4136	121.4021	121.4004
N(11)-C(1)-C(6)	117.3048	117.2997	117.3125
N(11)-C(1)-C(2)	126.0190	126.0215	126.0164
C(6)-C(1)-C(2)	116.6663	116.6741	116.6707

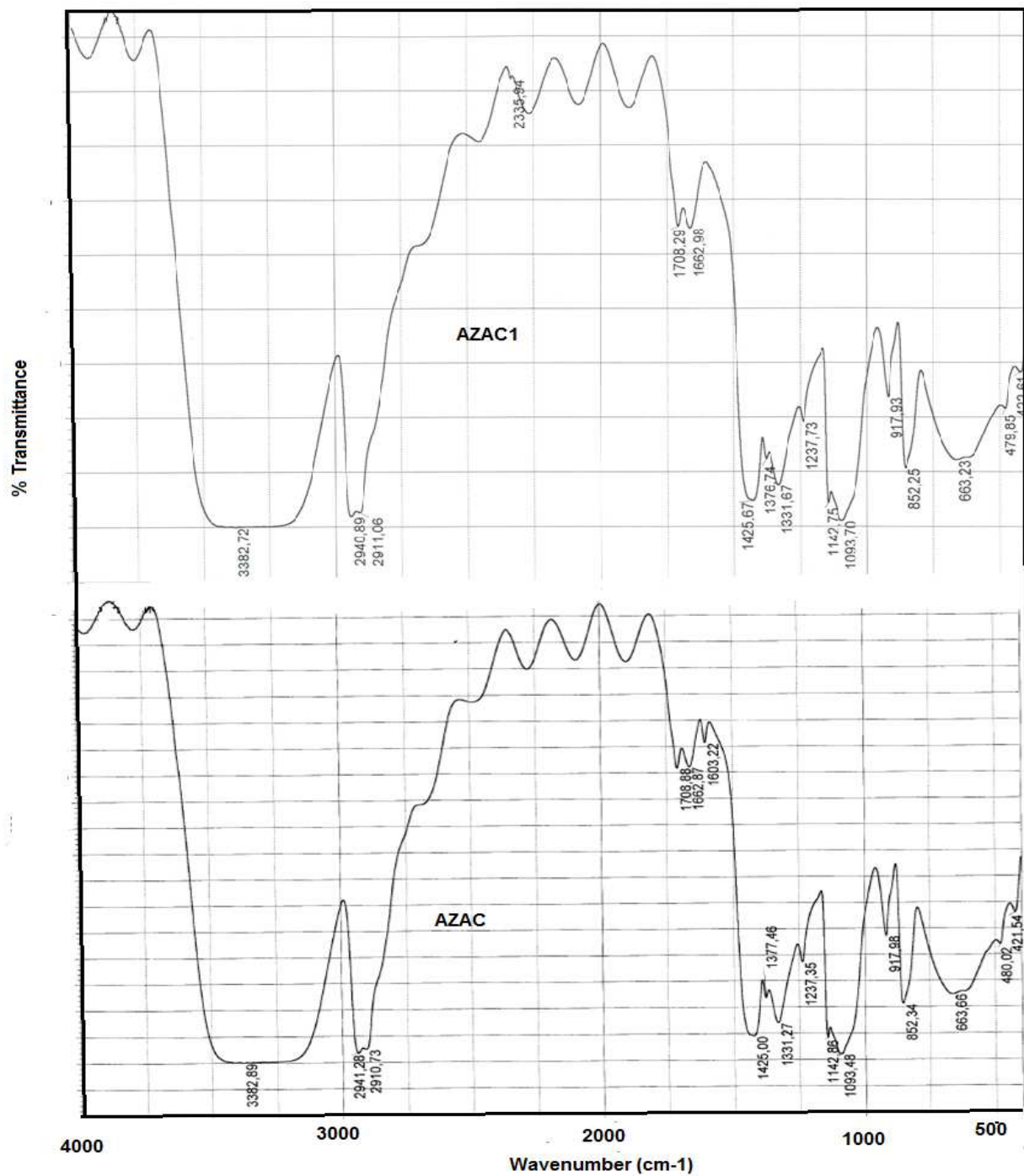


Fig. S3 Experimental IR spectrum of AZAC and AZAC1

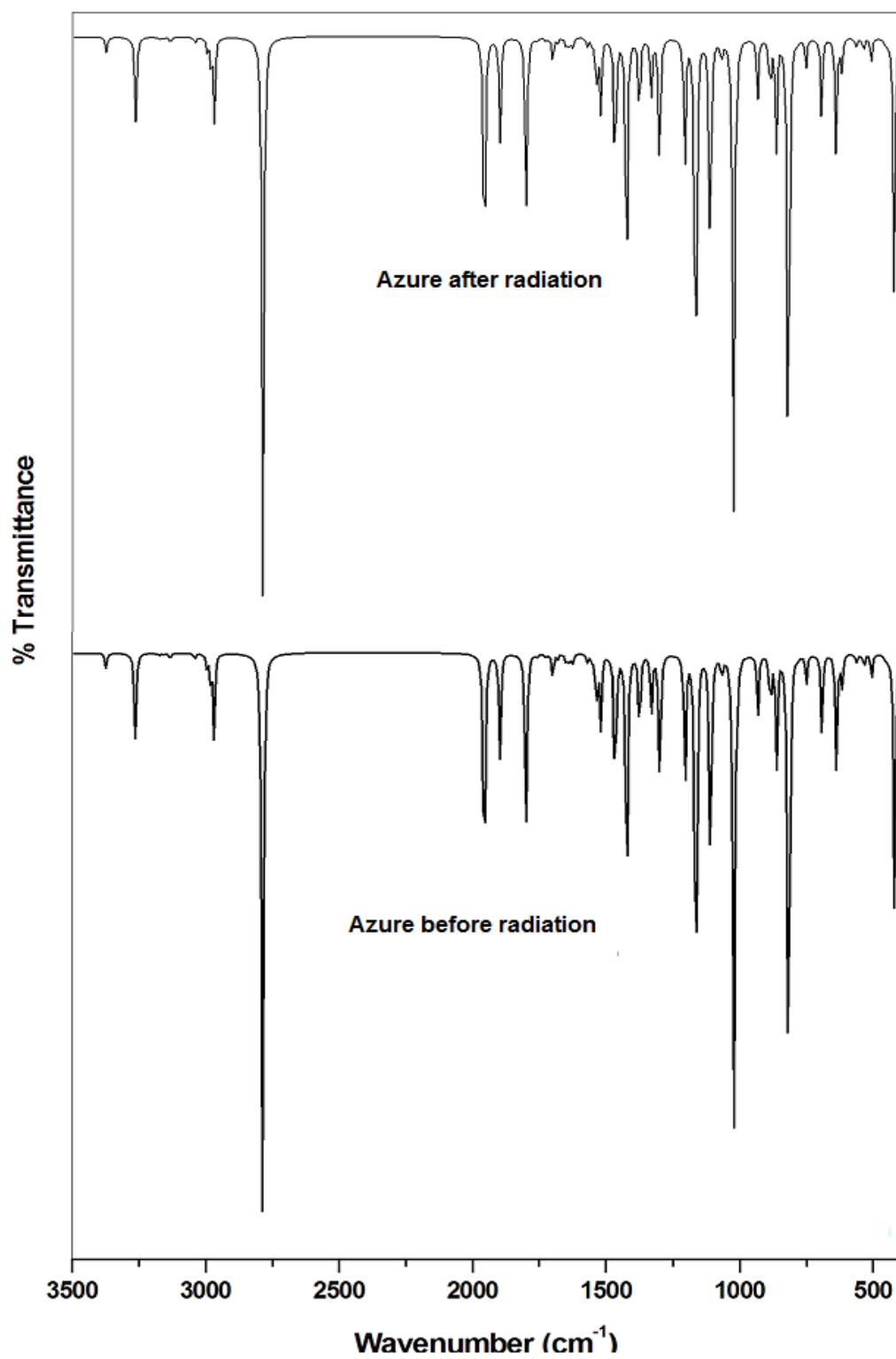


Fig. S4 Calculated IR spectrum of AZAC and AZAC1